Energies **2015**, *8*, 9009-9028; doi:10.3390/en8099009

OPEN ACCESS

energies

ISSN 1996-1073

www.mdpi.com/journal/energies

Article

Development of an Optimal Power Control Scheme for Wave-Offshore Hybrid Generation Systems

Seungmin Jung and Gilsoo Jang *

School of Electrical Engineering, Korea University, Seoul 136-713, Korea;
E-Mail: muejuck@korea.ac.kr

* Author to whom correspondence should be addressed; E-Mail: gjang@korea.ac.kr;
Tel.: +82-2-3290-3246; Fax: +82-2-3290-3692.

Academic Editor: William Holderbaum

Received: 28 May 2015 / Accepted: 18 August 2015 / Published: 25 August 2015

Abstract: Integration technology of various distribution systems for improving renewable energy utilization has been receiving attention in the power system industry. The wave-offshore hybrid generation system (HGS), which has a capacity of over 10 MW, was recently developed by adopting several voltage source converters (VSC), while a control method for adopted power conversion systems has not yet been configured in spite of the unique system characteristics of the designated structure. This paper deals with a reactive power assignment method for the developed hybrid system to improve the power transfer efficiency of the entire system. Through the development and application processes for an optimization algorithm utilizing the real-time active power profiles of each generator, a feasibility confirmation of power transmission loss reduction was implemented. To find the practical effect of the proposed control scheme, the real system information regarding the demonstration process was applied from case studies. Also, an evaluation for the loss of the improvement rate was calculated.

Keywords: hybrid generation system (HGS); reactive capability; reactive power assignment; power conversion system (PCS) control; voltage source converter (VSC)

---

1. Introduction

The growing interest in energy preservation in all industrial sectors has recently motivated the need to find sustainable technical solutions to reduce energy consumption. Nowadays, renewable energy sources are developed based on a geographically wide area and usually generate requirements for a management system to handle the entire system more appropriately [1]. Consequently, regarded industry areas have promoted the development of total control solutions, such as wind farm management systems, improving not only the mechanical conditions, but also the power control flexibility for the system operator [2,3]. In the case of the offshore generation industry, structural designs and integration studies have progressed by considering several different distribution systems including energy storage systems (ESSs) for increasing the reliability of the entire system's output profile [4,5]. Among these systems, an integrated system with various distribution sources, which is composed of an offshore cluster with some wind generators, has been receiving attention. These configurations have advantages in terms of efficiency as well as available energy quantity and, can lead to the reduction of construction costs by minimizing the related electrical systems.

In the case of the wave-offshore hybrid generation system (HGS), the configuration is suitable to increase the whole generation capacity with a number of distribution generators and the combined generation system can resolve the reliability issues of renewable sources [6]. In the current state of HGSs, several permanent magnetic synchronous generator (PMSG) wind turbines and permanent magnetic synchronous linear generator (PMSLG) wave generation systems have been built on a designed offshore platform, sharing various pieces of electrical equipment [7]. The electrical system's blueprint has almost been prepared but the optimized control logic has not yet been developed. General power control methods are available, but assigning an equivalent portion to several generation systems is counted as an inefficient solution. The HGS is intended to adopt a real time state monitoring system including power flow management, which can handle the power flow on a real time basis. The ongoing development of the central control algorithm would focus the utilization of the measured state of each system and find an optimal solution for the system's life cycle and operation efficiency. These countermeasures should include a wake effect analysis of wind turbines for considering active power efficiency and reliability, which are the main concerns of transmission and system operators (TSOs). Moreover, this type of large-scale generation system is responsible for reactive power support for the connected power grid, and integration of reactive/voltage management system to the conversion process is mandatory for utility grid. The most common distribution systems which have the reactive power supplying capability are the voltage source converter (VSC) interfaced generation system as mentioned in previous studies [8]. Active support by reactive power with VSC system has been continuously studied based on real/reactive power decoupled control considering own capability limitation [9,10]. An appropriate power flow management method by dealing with the above-mentioned issues is also considered as the final control form of HGS to offer a more appropriate required ancillary service for utility power grids.

In previous studies, only a real power assignment process has been considered due to the uncertainty regarding the environmental characteristics [11]. These considerations mean that the control logic of each generation system focuses only on the basic voltage reliability at each integration point (no responsibility for reactive power reserve) [12]. However, the HGS has unique characteristics in terms of the grid code because all requirements for the distribution system would be applied to the connection

point of HGS as a single generation system. The previous active power assignment methods usually applied on wind farms are not suitable for HGS because the composition of the two systems somewhat differ. Therefore, novel power assignment methods should be developed to make not only the control topology meets the specially designated grid codes but also the entire system improves own power efficiency.

This paper deals with a power assignment plan based on the composed real time monitoring system. By considering the output profile of the HGS, the optimized reactive power assignment process will be built to reduce the entire system loss. The structure of this paper is as follows: Section 2 describes the principles of HGS and the related management system. Section 3 explains the proposed optimization algorithm for minimizing system loss. Section 4 gives a verification process with the composed EMTDC simulation and Section 5 shows the arrangement of the proposed method and application process.

2. Hybrid Generation System (HGS) Configuration

2.1. Wave-Offshore Generation System

The concept of HGS is developed to reduce the platform construction cost and improve the utilization of power transfer equipment [13,14]. The entire capacity of the system has increased over than 10 MW in terms of power capacity and the total area of the floating structure is expected to be over 40,000 m^2. All of the main generators are built on the floating structure and the required electricity devices also located inside the floating structure. Three MW PMSG wind turbines will be located at each vertex of the structure and 24 wave generators are erected at the corner of the structure to generate a 2.4 MW power profile. The total capacity of the recent HGS is 14.4 MW and the power conversion system (PCS) of the wave generator is shared by a number of generators. Figure 1 shows a conceptual image of the HGS. In the structure, several transmission cables are installed, and integration points occur at the center of each specific row. The AC cable is used for the wind power system and wave generators are installed at a single DC section based on the low voltage DC distribution system [15]. With the integration point as the center, a system can transfer generated energy to a center substation, which is responsible for following the reference signal by TSO.

The substation including DC/AC PCS is located in the central station to boost the primary voltage to the transmission level for integrating the HGS with the point of common coupling (PCC) through a high-voltage condition. Another main role of the central station is to act as a monitoring system for measuring the real-time condition of each system to manage the entire HGS for an optimized state. Especially, since all of the generation systems in the HGS utilize a VSC, studies on the appropriate voltage regulation method focusing on the PCC are being carried out. This paper deals with advanced reactive power control with an integrated monitoring system. The HGS first considers the wake effect of the wind system to achieve maximum power point tracking (MPPT) continuously and the proposed control scheme would make the reactive power assignment process efficient through developing an optimization process. In particular, the reactive power reserve would be maximized if we consider the output power of the entire system in a real time basis, and it will be the main strength of the proposed system.

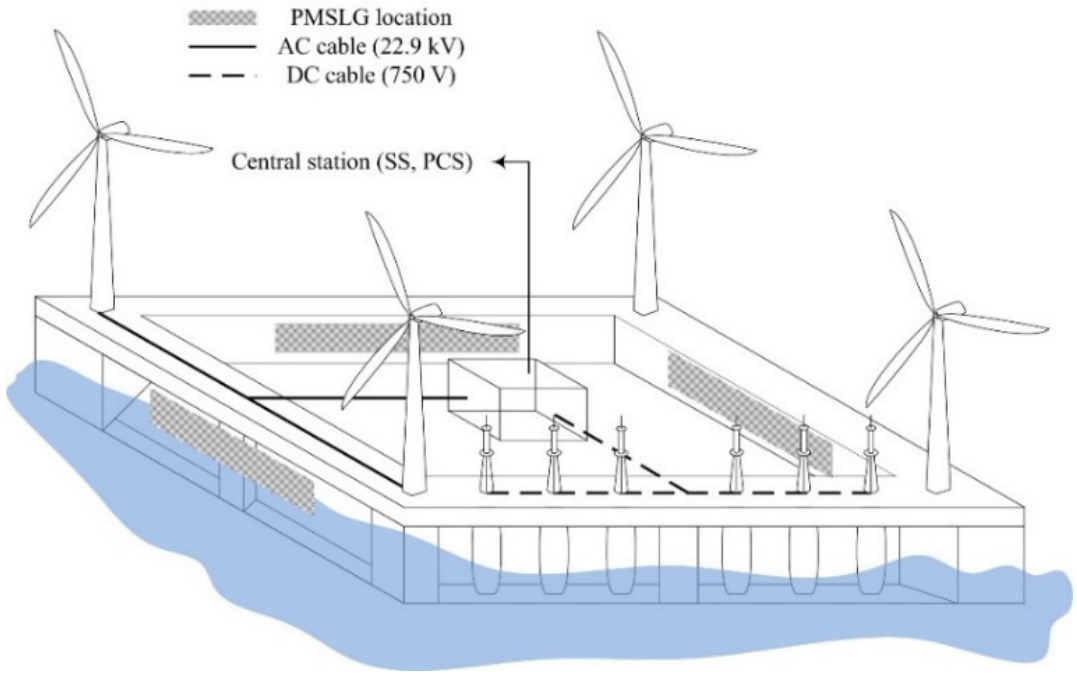

Figure 1. Concept of the wave-offshore hybrid generation system (HGS). PMSLG: synchronous linear generator; PCS: power conversion system.

2.2. Integrated Monitoring System

Since the power capacity of the composed HGS is significantly greater than that of the previous renewable sources, a further management solution should be considered for the system to improve reliability and the individual ancillary service. By focusing on the profile at the connection point of the HGS, the order of TSO for an active/reactive power signal should be controlled for matching the system requirement.

As a countermeasure to this issues, the HGS introduces a supervisory integrated monitoring and control system (IMCS) that can check the state of the system continuously, not only the mechanical load of each structure, but also the electrical conditions including voltage level and active/reactive output. The control signal for each generation system would be formulized based on the TSO orders and modified according to the output profile of the central transformer. In the case of active power, the wind turbines usually follow MPPT control and the profile exceeded above the reference could be limited thorough a supervisory control system with individual mechanical properties such as pitch control. The wave generation system does not adopt the power limitation method and is designed to follow the MPPT process continuously. On the other hand, reactive power could be controlled by applied full-type conversion systems of the wind system according to the operator's purpose, and this could enhance the HGS in term of a controllable reactive power capacity. Furthermore, the wave generation system also adopts a common converter system that includes a 2.4 MVA grid-side voltage source DC/AC inverter. These reactive sources can maximize individual reactive power capability by utilizing the output profile information on a real time basis. Because the available reactive power of the full-type converter depends on the profile of the active power of each generation system, it is worthwhile imposing these values in the power control scheme if the TSO demands more reactive power than the previous state. Above all, matching output profile with the active/reactive power order of the operator is obligated to these

large-scaled power generation systems even for the systems with renewable sources [16], the importance of supervisory control will be growth, and the future power control scheme will focus to utilize the obtained information.

2.3. Wind System Characteristics

The wind systems in HGS were designed to obtain the real power from the wind resources of the prevailing wind direction, which is considered the main energy of HGS. However, the prevailing wind direction cannot be maintained continuously during the system operation, and the wake effects inside HGS should be analyzed appropriately to cope with the mentioned condition. The wake effect is not generally considered when the distance between each wind turbine is greater than the designated value [17]. However, for the HGS that includes a wind system having a relatively short distance among installed wind turbines, a significant wind speed reduction is expected when the changed wind condition is applied. Figure 2 presents the necessity of the proposed power control scheme. Almost all of the output profile of the wind system would be obtained from the prevailing wind direction, and the other wind direction (yawing control required) would normally not be considered; nevertheless, the actual wind energy reduction and related fluctuation occurs according to the previously analyzed effect when the wind passes through the front line of the wind system. If the HGS changes the status and confronts the mentioned situation, a significant gap of real power profile obtained from encountered wind energy occurs between the wind turbines of the front array and the wind turbines of the rear array.

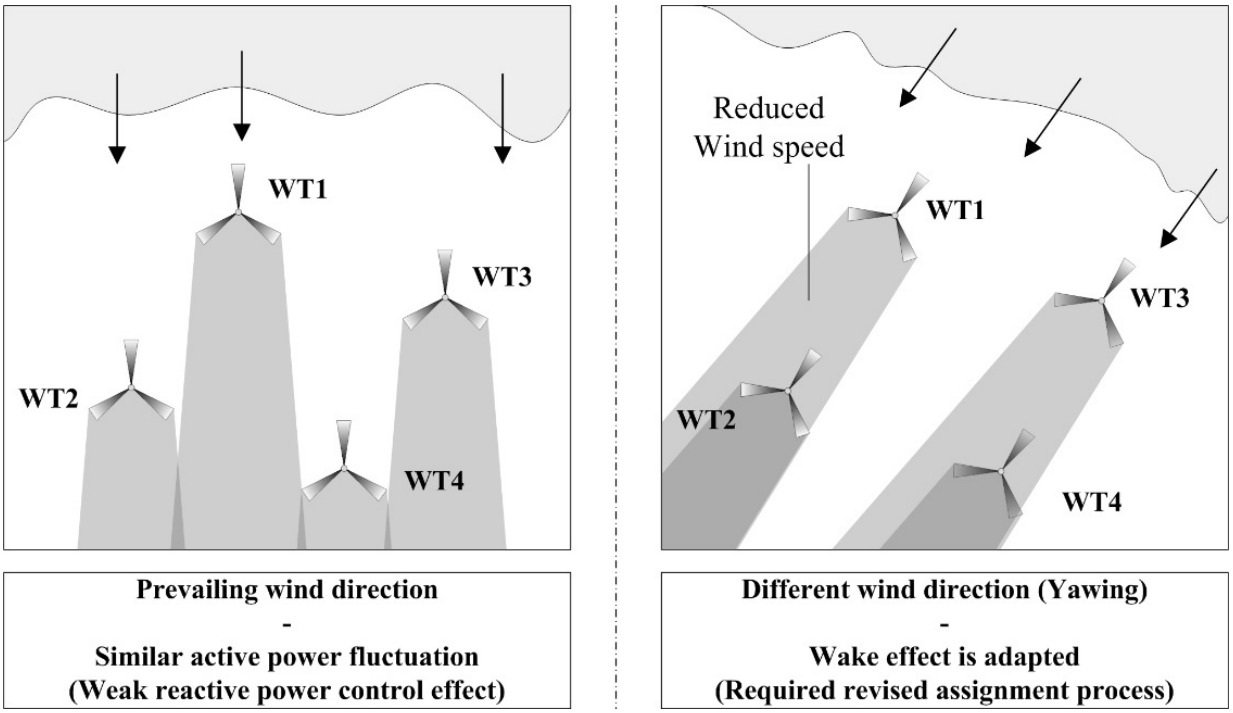

Figure 2. Target situation regarding wake effect.

Figure 3 shows the mentioned situation where the system confronts the entire wake effect. The applied wind speeds at the wind turbines of the rear array are significantly reduced. With this condition, the active power outputs of each wind turbine differ significantly.

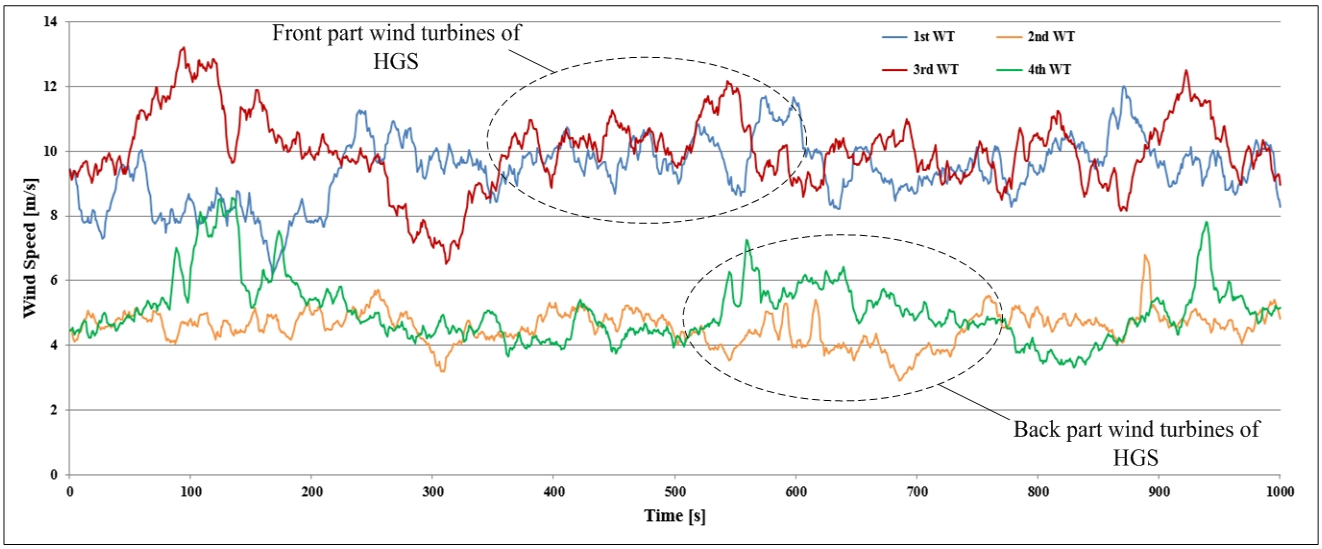

Figure 3. Different wind resources applied to HGS.

These differences could generate current and voltage different in the electrical system, which are related to the transfer efficiency. Hence, these current flow differences due to the active power demand further valancing control of the reactive power. Especially, since the duty of the reactive power supply of HGS is fully determined with the common coupling point, the current flow minimization ability of the inner system can result in a fine solution for the HGS (the requirements are achieved if the total reactive power output is equal to the designated value by TSO). To achieve this, the designed reactive power assignment process will use the real-time measured value obtained from the integrated management system and the purpose of this process is to minimize the current flow for the electric cable in HGS.

When the entire system utilizes the power control method and applies it in the PCS management system, the active power loss due to the active power difference could be mitigated continuously. The IMCS will transfer the required values to the management system by using individual measuring devices, softening the operation of the algorithm's interworking.

3. Power Control Algorithm

3.1. Proposed Method Description

The aim of the proposed algorithm is to assign reactive power requirements by focusing on the measured online active power profile of each wind turbine. The certified reactive power quantities are assigned through several stages by considering each device's current state. First, the unusual system structure of HGS is a major consideration for the assignment process because TSO does not consider each unit in the HGS as an individual controllable unit and the management system can control the available power according to the designed flow chart. The loss improvement can be achieved by considering the system layout because the components of the cable directly influence the loss occurrence. Additionally, the method should check the difference between the cable parameters of each section because the determination of cable specification depends on the expected current flow from each generation unit.

Figure 4 shows the electrical system structure that was mainly analyzed in the proposed process. Since the electric cable parameters of each section are different, several loss expectation formulas need to be included in the reactive assignment method to achieve the optimization process. Two classified sections, named "array", will be interconnected with the center substation through a thicker electric cable than the individual electric cable of the wind turbine. The proposed method first focuses on establishing a proportional equation at each section in relation to reactive power by using designated cable components. The cable parameters used in the HGS are shown in Table 1. This values will be imposed to controller before operation and utilized in loss expectation process. The wind turbines on the connection point (marked at the Figure 4) are classified with two different turbine "A" and "B". In Section 3.2, assignment equations are formulized with this classification. The configured formulas could be applied to different connection points through the divided calculation mode with an additional consideration such as voltage fluctuations.

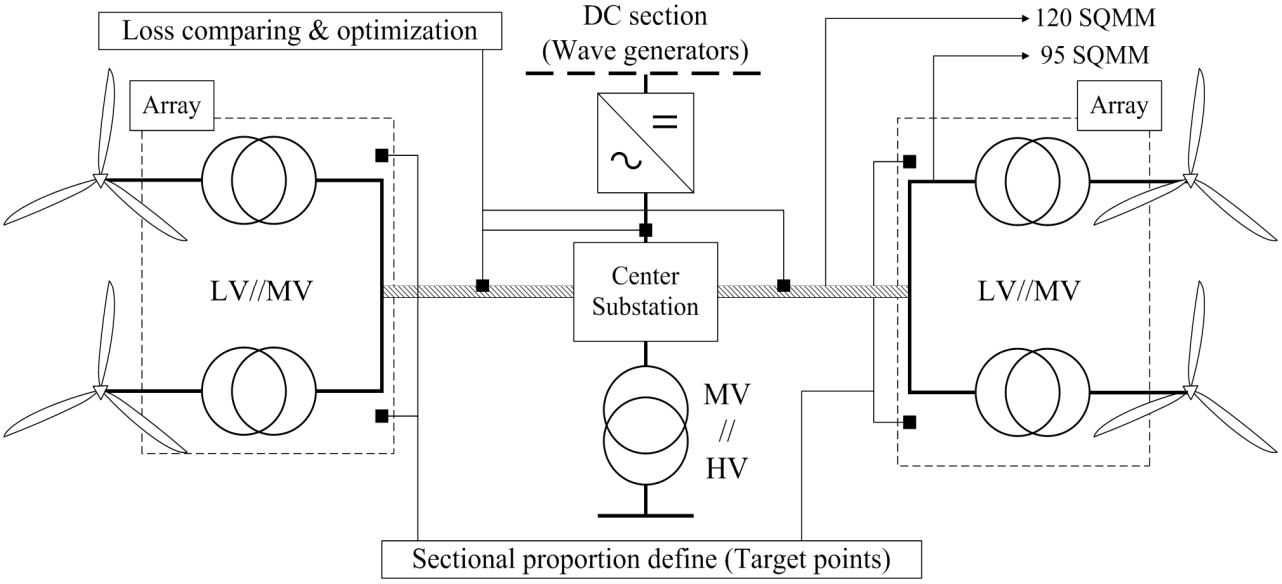

Figure 4. Electrical system structure of HGS and control purpose description.

Table 1. Numerical cable parameter in HGS.

Voltage (kV)	Size (mm^2)	Allowable current (A)	Conductor resistance (Ω/km)	Inductance (mH/km)	Capacitance (μF/km)
0.75 (DC)	35	228	0.565	0.277	0.08
	50	289	0.393	0.266	0.09
22.9	95	291	0.193	0.42	0.17
	120	330	0.153	0.41	0.18

The following section will discuss the loss equation. The general assignment process that can be applied to each point will then be introduced. The proposed decision process for the proportion focuses on the current balance of a certain section according to the current output of wind turbines. When the proportion of the reactive power is designated with the measured active power, the main system can calculate the expected loss including the wave generation system. By comparing the expected loss according to the assigned quantity, the algorithm can set the reference signal of the reactive power.

Through the designed process, loss expectation and minimization could be performed by balancing the current flow of each section.

3.2. System Loss Equation

To obtain the loss reduction process, a real power loss equation should be built in each section. Figure 5 shows the system structure of HGS by dividing it into several sections to illustrate the mentioned equations. Each generation system demands an electric cable that would be located on the outer deck of HGS. Basically, every outer deck will include a DC cable for the wave generation system. Additionally, AC cables for integrating wind turbines would be included in some of the outer decks.

The wave generation system utilizes a linear generation system and the generated power would be transferred to the center power system in a DC electric form by using an individual AC/DC converter [18]. Because the DC current would change in the AC form at the center of the power station, the represented DC section in the figure is operated as a type of low voltage distribution system. In this paper, because we focus on the active/reactive power flow on the AC system, the AC cable structure and related cable information should mainly be discussed. There are two arrays (grouping two wind turbines as one array) in the HGS and both arrays are interconnected with center substation to transfer the controlled output value to the utility grid.

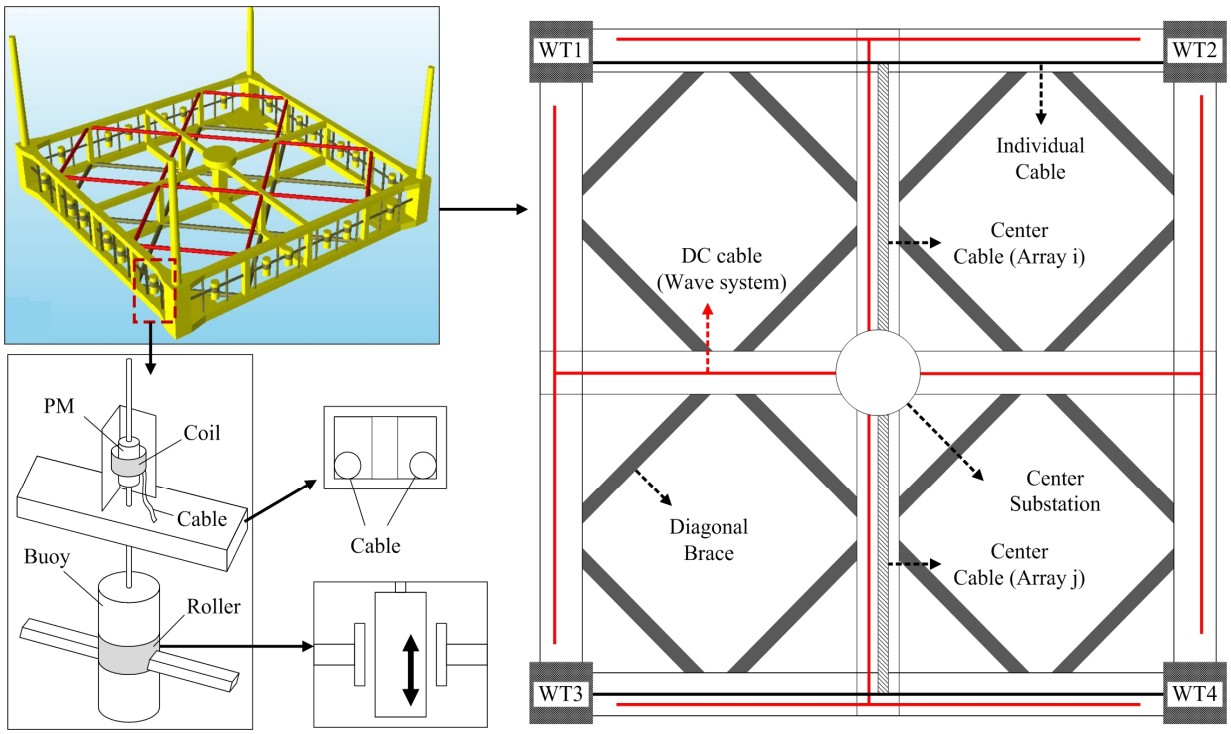

Figure 5. HGS structure analysis-electric cable location.

Basically, the distance between connected wind turbine and the center cable is the same; therefore, the loss occurring in the two cables fully depends on the power flow states. Since the power control station is directly interconnected with a dedicated line, the entire profile of the real system could be defined as Equation (1):

$$P_{\mathrm{HGS}} = P_{\mathrm{wave}} + P_{\mathrm{wind}} \tag{1}$$

where P_{HGS} is the real output power of the entire HGS, P_{wave} is the real output power of wave generators, and P_{wind} is the real output power of wind turbines.

The output profile of total wind system could be divided into the each turbine's output value and each section's loss term. Equation (2) shows the divided quantity, and the loss of a certain array could also be divided as shown in Equation (3) by using the terms defined above:

$$P_{\mathrm{wind}} = \sum P_{\mathrm{wt}} - \sum P_{\mathrm{L}} \tag{2}$$

$$P_{\mathrm{L}} = P_{\mathrm{L\cdot CNT}} + \sum P_{\mathrm{L\cdot IND}} \tag{3}$$

where P_{wt} is the measured output power of the wind turbine, P_{L} is the system loss at a certain array, $P_{\mathrm{L\cdot CNT}}$ is the system loss by the center cable, and $P_{\mathrm{L\cdot IND}}$ is the system loss by the individual cable.

If we assume that a wind turbine can precisely generate reactive power according to the reference signal, the loss equation can be created directly. The real loss at a certain array can be composed of two individual loss equations as follows:

$$P_{\mathrm{L\cdot CNT}} = r_{\mathrm{CNT}} \cdot \frac{\left(\sum P_{\mathrm{wt}}\right)^2 + \left(\sum Q_{\mathrm{ref}}\right)^2}{V^2} \tag{4}$$

$$P_{\mathrm{L\cdot IND}} = r_{\mathrm{IND}} \cdot \frac{{P_{\mathrm{wt}}}^2 + {Q_{\mathrm{ref}}}^2}{V^2} \tag{5}$$

where r_{CNT} is the resistance of the central cable, r_{IND} is the resistance of the individual cable, and Q_{ref} is the reactive power reference of a certain wind turbine.

According to the above equation, the sectional loss is dependent on not only the active power, but also the reactive power. Therefore, the current control can be achieved with a reactive assignment process by considering the active power variation. The voltage variation at the connection point can normally be neglected due to the continuous regulation by the full-type converters in the wind turbines. However, owing to the significant power fluctuation or system fault, the voltage gap can be too high to ignore in some cases. The proposed method considers both conditions and divides the calculation process into two classified assignment processes.

3.3. Reactive Power Assignment Method

As mentioned above, the total reactive power order for HGS is specified by TSO as a single distribution source. Therefore, the inner control system could designate the appropriate value to each system to match the output profile with the order. The total value of the reactive power reference is shown in Equation (6) and the reference signal for wind system can also be divided into each array as shown in Equations (7) and (8):

$$Q_{\mathrm{order}} = Q_{\mathrm{wave}} + \sum Q_{\mathrm{array}} \tag{6}$$

$$Q_i = Q_{\mathrm{ref1}} + Q_{\mathrm{ref2}} \tag{7}$$

$$Q_j = Q_{\mathrm{ref3}} + Q_{\mathrm{ref4}} \tag{8}$$

where Q_{order} is the reactive power order designated by TSO, Q_{wave} is the reactive power order for wave generators, Q_{array} is the reactive power order for array, Q_i is the total reactive power reference of array i, and Q_j is the total reactive power reference of array j.

The established formulas will be applied at a connection point for assigning the designated reactive power quantity to the two different turbines named A and B in the above section. Considering the voltage variation level, the assignment processes are classified according to the two following processes.

3.3.1. Low Voltage Variation

Normally, the AC voltage levels at all sections in the HGS are almost the same because the scale of the entire system is small to cause a large voltage difference. In this case, the voltage level in Equations (4) and (5) could be neglected in the loss comparison process (V = 1.0 p.u.). Furthermore, since both resistance values in all assignment points are equal due to the structural characteristic, matching the two expected losses could be represented in Equation (9):

$$P_A^2 + Q_A^2 = P_B^2 + Q_B^2 \tag{9}$$

where P_A is the measured active power output of turbine A, P_B is the measured active power output of turbine B, Q_A is the required reactive power quantity of turbine A, and Q_B is the required reactive power quantity of turbine B.

As the active power value is continuously checked and utilized as a constant value, the reactive power quantity of each wind turbine could be calculated directly by using Equation (10). With this value, the reactive power flow will be modified according to the active power flow by wind turbines. To prevent a negative reference signal due to the low reference quantity by the upper process, the modification processes were established in Equations (11) and (12) as follows:

$$Q_A = \frac{(Q_{array})^2 + P_B^2 - P_A^2}{2Q_{array}}, \quad Q_B = \frac{(Q_{array})^2 + P_A^2 - P_B^2}{2Q_{array}} \tag{10}$$

$$Q_A = Q_A - |Q_B|, \quad (Q_B < 0) \tag{11}$$

$$Q_B = Q_B - |Q_A|, \quad (Q_A < 0) \tag{12}$$

These equations are applied to find a solution to the inner-array assignment process. The current flow of each cable in the HGS could be more balanced than with the proportional distribution method, increasing the power transfer efficiency. The voltage variation for selecting the assignment mode would be checked for every calculation state, and if the variation is higher than the designated value, the following assignment process will be performed.

3.3.2. Considering Voltage Variation

If the voltage variation is increased due to the abnormal condition, the voltage level of each point should be considered. The voltage condition is checked by IMCS and transferred to the main control algorithm to determine whether or not the variation is considerable. If the value is high and can generate error in the calculation process, the voltage value will be imposed at the current balancing process. As the above section's assignment process, these calculation processes also consider two different points

as an assignment required section. By adapting the above equation including voltage values, the reference of a certain point could be designated in Equation (13):

$$Q_{\mathrm{A}}^2 = \left(\frac{V_{\mathrm{A}}}{V_{\mathrm{B}}}\right)^2 \cdot Q_{\mathrm{B}} + \left(\frac{V_{\mathrm{A}}}{V_{\mathrm{B}}}\right)^2 \cdot P_{\mathrm{B}}^2 - P_{\mathrm{A}}^2 \tag{13}$$

where V_{A} is the measured voltage of turbine A and V_{B} is the measured voltage of turbine B.

Since the sum of the required reactive power of each point should match the reactive power order, the designated reactive power quantity of the certain connection point can be represented as follows:

$$\left[\left(\frac{V_{\mathrm{A}}}{V_{\mathrm{B}}}\right)^2 - 1\right] Q_{\mathrm{A}}^2 - 2\left(\frac{V_{\mathrm{A}}}{V_{\mathrm{B}}}\right)^2 Q_{\mathrm{A}} Q_{\mathrm{array}} + \left(\frac{V_{\mathrm{A}}}{V_{\mathrm{B}}}\right)^2 P_{\mathrm{B}}^2 - P_{\mathrm{A}}^2 + \left(\frac{V_{\mathrm{A}}}{V_{\mathrm{B}}}\right)^2 Q_{\mathrm{array}} \tag{14}$$

By solving Equation (14), two reference values for each turbine can be calculated. The modification processes in Equations (11) and (12) are equally applied in this process. With the allocation process, the loss expectation of HGS could be directly determined.

3.3.3. Incremental Loss Comparison

To achieve the loss minimization process, an incremental loss calculation process can be performed as follows:

$$\frac{\mathrm{d}Loss}{\mathrm{d}Q_i} = \frac{\mathrm{d}Loss}{\mathrm{d}Q_j} = \frac{\mathrm{d}Loss}{\mathrm{d}Q_{\mathrm{wave}}} = \lambda \tag{15}$$

The minimized power loss by reactive power can be calculated with the incremental loss. When the incremental losses of each part are equal, the references quantity of the wind and wave system is designated and it will be available in the control processes. Then, the reference signal for each generator could be designated as follow above equation. Figure 6 shows the flowchart of the entire assignment process.

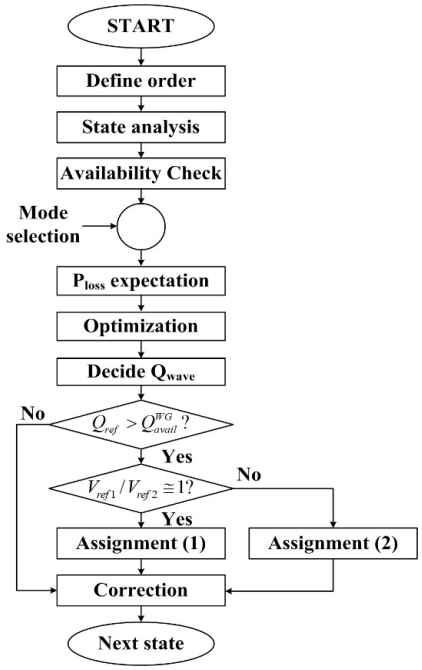

Figure 6. Introduced entire allocation process.

The IMCS first checks the current status and system requirements to confirm the availability of the reactive power control. The capability curve for checking the reactive power reserve depends on the composed conversion system specification and the designated power factor (PF) as Equation (16). The operator could determine the available reactive power quantity using the real power output with the power conversion capacity as defined in Equation (17):

$$|Q_{\max}| = \sqrt{1 - PF^2} S_{\text{cap}} \tag{16}$$

$$|Q_{\text{ava}}| = \sqrt{S_{\text{cap}}^2 - P^2} \tag{17}$$

where $Q_{\max}$ is the maximum reactive power capability and S_{cap} is the power conversion capacity of the converter (MVA) Q_{ava} is the available reactive power.

The reactive power control would then be performed according to the designated control mode to reflect another system requirement. In the next stage, the power loss due to the reactive power reference for each section (array 1, array 2, wave generation system) will be calculated with the above assignment process. The loss expectation can be easily carried out with the assigned formulas because the reference signal for each system will be designated with the mentioned linear components of HGS. With the measured active power profile by IMCS, expecting loss, and finding the optimized value for incremental values can be accomplished. Finally, the reference signal for the PCS of the wave generation system will be designated and an optimized solution can also be found for the wind system.

4. Simulation

4.1. System Design

To verify the proposed power control algorithm, the HGS was configured with EMTDC simulation. A 3.3 MVA PCS is utilized to integrate three MW PMSG wind turbines, and the wave power generation system adapts 2.4 MVA PCS to change the individual electrical form of the output profile. The whole PCS was configured with full switching modules. Figure 7 presents the configured PCS in the HGS. Four wind turbines were connected to the grid through a 3-level neutral point clamped (NPC) voltage source inverter [19]. The 4 rotor-side convertors follow MPPT control independently, and the reactive reference currents are also controlled by the individual grid-side convertors utilizing the system states pulled by the phase locked loop and order of the system operator. In order to capture the maximum power from encountered wind, P-ω relation applied look-up table which predefines the points of maximum aerodynamic efficiency is contained. The wind system will generate optimized power according to the maximum power coefficient (c_{opt}) during the simulation. Taking into account the system specification, the wave generation system has adopted two level PCS modules. Also, the VSC for wave generators have previously been configured with individual generator-side converters and a single common grid-side convertor, but in this paper, both PCSs were applied to a single PCS by combining 24 wave generators to reduce simulation complexity. Except for generating the switching signal, both power control modules utilize the measured grid information and follow almost the same topologies.

The converter control is divided into generator side control and grid side control. Since the reactive power supply to the grid is independent from the reactive profile of generator, reactive power orders for the grid side converter including system limits are mainly treated in this paper and the wind power system

including mechanical values will follow the referred previous studies. In the current reference designation process, the capability limitations are applied to impose both system's configuration. The generated signal is used to generate a set of three-phase reference voltage to control pulse width modulation (PWM) converter.

The EMTDC simulation for analyzing the proposed algorithm was configured by utilizing real wind data that applied the full wake effect. In the simulation, the wind speed was applied to the turbine with a time-table form. The back part wind turbines would encounter a reduced wind speed compared to the previous state. The reactive power signal for system electrical efficiency could be verified through the designed system.

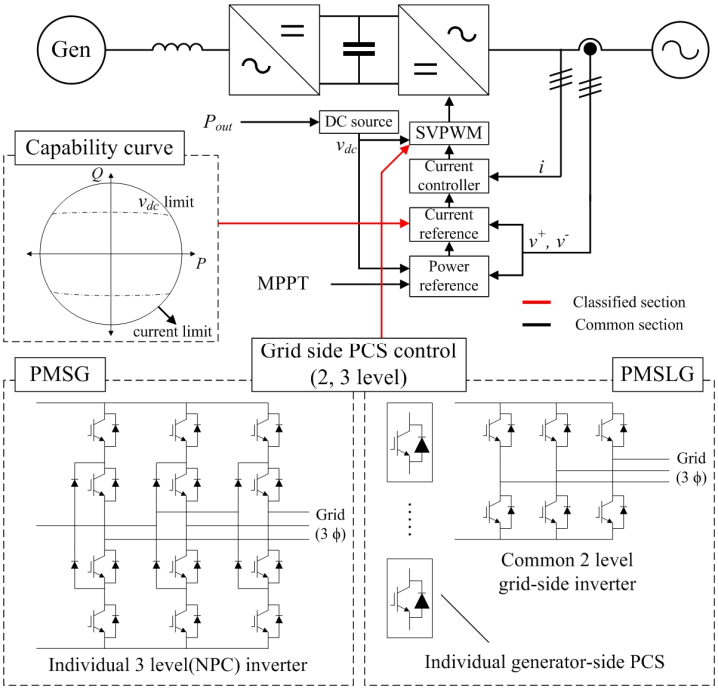

Figure 7. VSC control concept of HGS in the simulation.

The case studies could be verified by designing a feed-back loop to match the reference signal for the reactive power with a real output profile. For appropriate handling the voltage/reactive power according to the real-time variation value, the system profile should be included in the control process (a PI control scheme was added to the reactive power control and performed for each case study).

4.2. Simulation

In order to estimate the proposed method in terms of system efficiency, PSCAD/EMTDC simulation was performed with the realistic power fluctuation condition. The wake analysis result was implemented through the PSCAD/EMTDC simulation for demonstration. To confirm the suitability of the proposed method, not only the efficiency regarding power loss but also the absorbed reactive power flow at PCC need to be verified. Especially, the grid connection requirements should be satisfied regardless of the dynamic power fluctuation according to the wind resources. Figures 8 and 9 show the active power profile of the HGS by dividing the wind generation system and the wave generation system. The entire simulation time is 25 s and the front wind turbine is designated to WT1 and WT3.

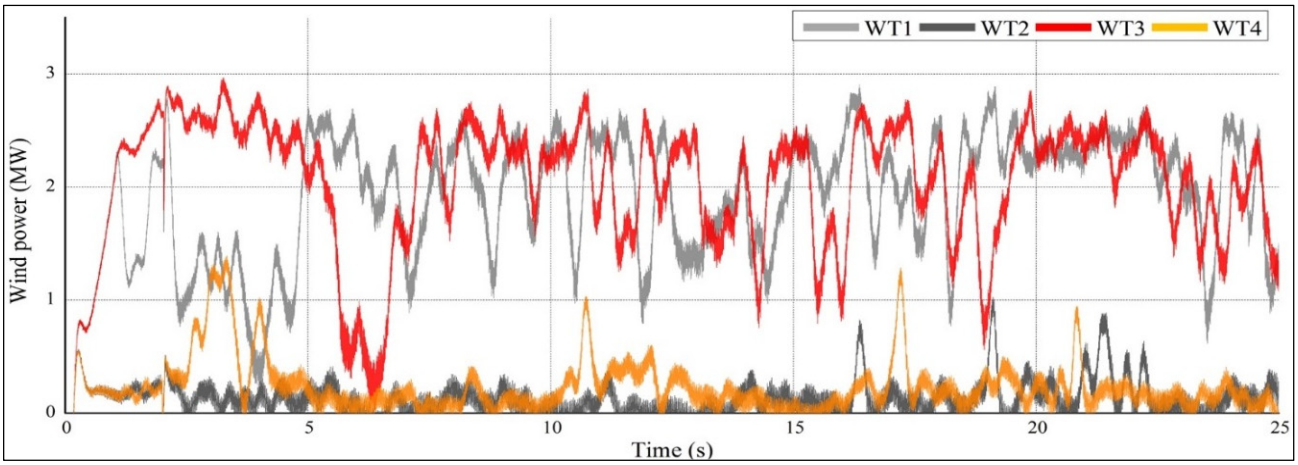

Figure 8. Wind power fluctuation in the designed case studies.

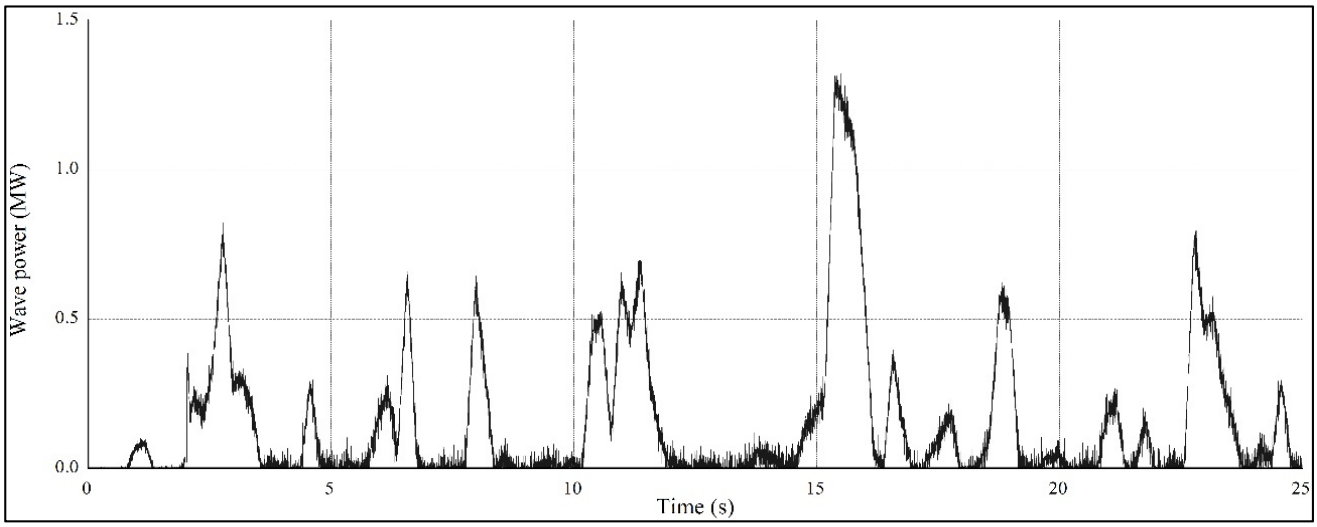

Figure 9. Wave power fluctuation in the designed case studies.

As shown in the mentioned structure (Figure 5), the wind turbines in the simulation were electrically integrated with the central power system through designated cable components. The cable data in Table 1 are utilized in the simulation.

In order to check the control effect and the following state, a caparison between normal and adapted control was equally carried out for the above power generation condition. Table 2 represents the simulation parameters of the designed system in this paper. As mentioned above, the wave generators are comprised of a DC system and are connected with the single PCS in the center of the station. The equivalent source is incorporated by considering the short circuit ratio (SCR), which is used to estimate the system's robustness. Order changes during the simulation are represented in Table 3. In the simulation, the required reactive power changes from 0 MVar to 4.73 MVar (0.95 lagging power factor of entire capacity of HGS). The cases that applied the proposed algorithm are divided into two different simulations for confirming the feasibility of the capacity limitation which is represented in Equation (16). The representative simulation was designed without considering reactive power capability limitation. The simulation of designating maximum reactive power reserve with 0.9 PF was also progressed in the below section. After a short initializing section, the proposed control scheme is applied to the system.

Table 2. Numerical data of the performed simulation.

Number (*n*)		Rate power (MW)			Grid data		WT-WT distance	Simulation time
WT	WG	WT	WG	Total	SCR	X/R	(m)	(s)
4	24	3	0.1	14.4	15	15	100	25

Table 3. Reference signal for case studies.

Case	Initialize section (s)	Normal control (s)	Proposed control (s)	*Q* order (MVar)
Non-adapted	0–2	2–25	-	4.73
Adapted	0–2	2–3	3–25	4.73

Figure 10 shows the original reactive power curves of the wind and wave generation system in the case study. Every generation system is given the same reference signal by the system operator and generates reactive power equally. Although slight differences exist between each generator due to the electrical condition, the overall output characteristics are constant during the simulation. In the adapted simulation case that represented in Figure 11, however, the reactive power output continuously changes during the simulation. After applying the algorithm at three second, the conversion system automatically imposes calculated reference value; hence the graph indicates the new power curve with the proposed algorithm for the same time period and operational condition. The reactive power curves show opposite characteristics which is contrary to the generated real power as shown in Figure 8.

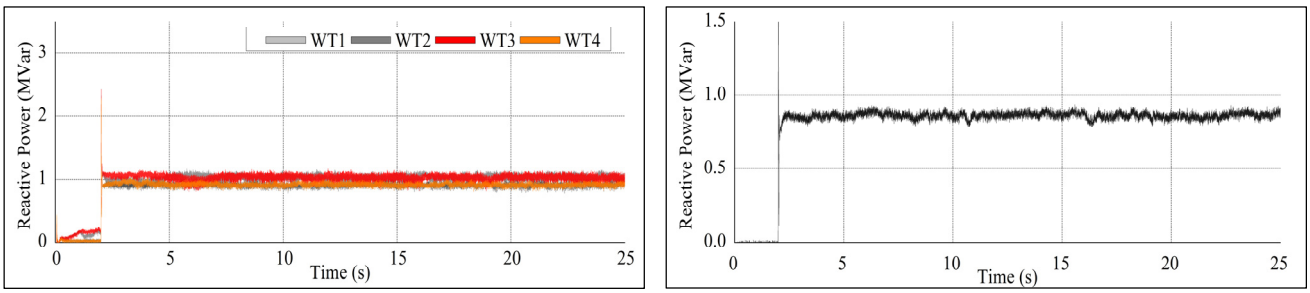

Figure 10. Reactieve power output with normal proportional control: (**a**) wind turbines; and (**b**) wave generation system.

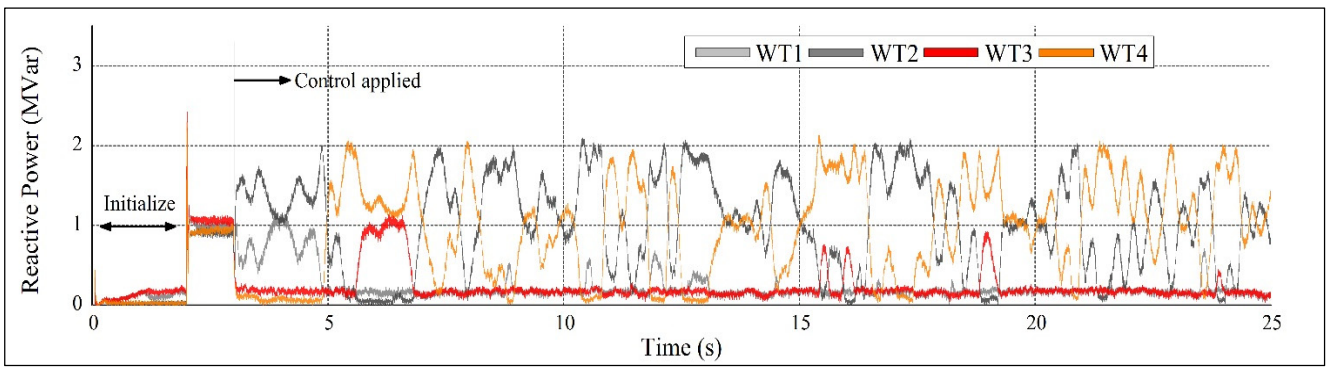

Figure 11. Reactive power output with proposed control-without capability limit (wind turbines).

As shown in the reactive profile curve of Figure 12, the proposed algorithm was performed ordinarily with capability limitation designated by system operator. Although the opposite characteristics about real power is not imposed rather than Figure 11, the fluctuation still follow the current minimization process. The reactive power profile of each generator is adjusted to reduce the apparent power flow in the cable. Not only the wind power but also the wave generation system participates in the control scheme.

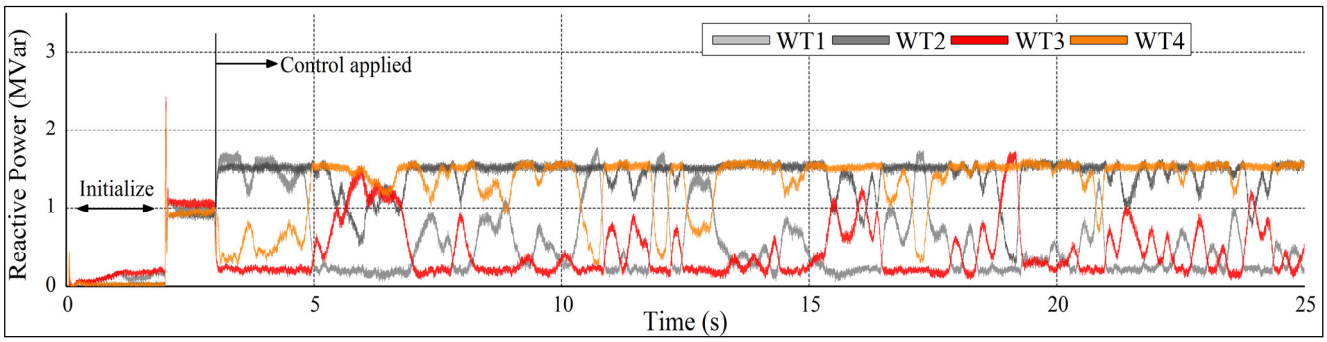

Figure 12. Reactive power output with proposed control-with capability limit (wind turbines).

Figures 13 and 14 show the reactive power fluctuation of the wave generation system with proposed control method. Conversion systems were performed according to the calculated signal by the mentioned formulas, and no measured errors were observed in the simulation using a full scale switching model. Without reactive power capability limit, the converter for wave generation system is fully utilized and the active power change directly affect the reactive power fluctuation. In case of limit-imposed simulation, however, pre-calculated maximum quantity of reactive power regulate the utilization of the applied conversion system.

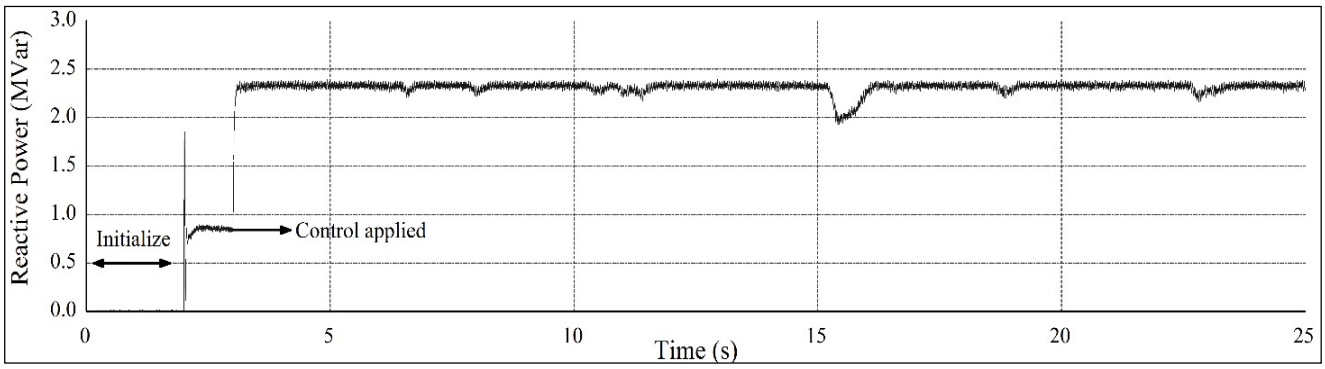

Figure 13. Reactive power output with proposed control-without capability limit (wave generation system).

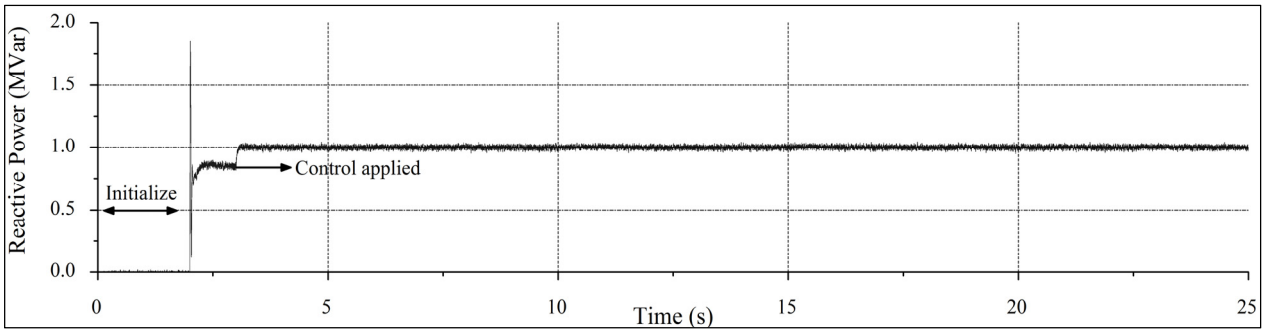

Figure 14. Reactive power output with proposed control-with capability limit (wave generation system).

In order to check the system impact and improvement in terms of system loss, two graphs are shown in Figure 15. The system has continuous reactive power fluctuation during the control process, but the absorbed reactive power at PCC is not affected. At PCC, the reactive power absorption between the two control schemes does not differ, as shown in Figure 15, even if the control method changes. The proposed controls show similar output characteristics in terms of reactive power supply. As shown in the Figure 15b, both curve stably supply reactive power and the averaged quantity is same with the normal operation. Mitigation of the energy loss in the system is depicted in Figure 16, due to the reduction of current flow. The averaged system loss of both methods, the energy loss in the simulation, and the absorbed reactive power at PCC are presented in Table 4. The loss reduction percentages are slightly over 6% and the improved power profile quantity is larger than 0.1 kW/s. Since the energy loss was measured during the entire simulation, the percent improvement value slightly differs with that of power loss. Even if the improved quantity of power loss is not significant, the annual production improvement (assumed to 919.8 kWh) can be a considerable benefit to the system owner. As the reactive support request from utility grid is growing, the impact could be significant than expected state. Moreover, the measuring and integrating processes of precise reactive power reserve will improve the active support plan regarding voltage/reactive power management methods.

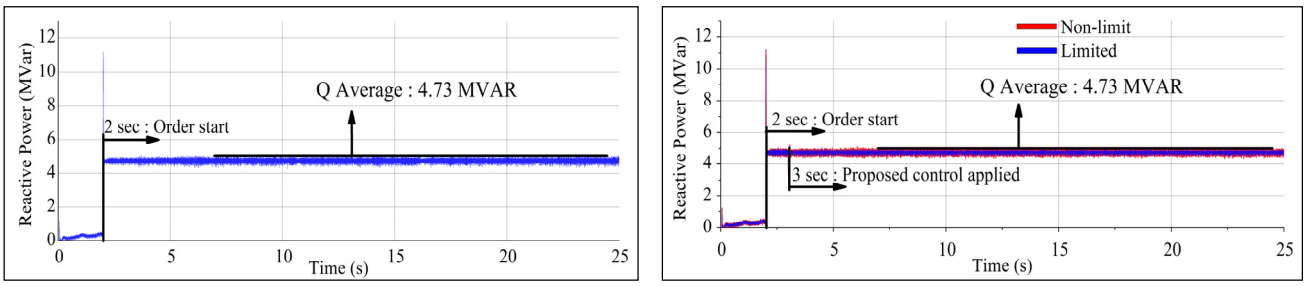

(**a**) (**b**)

Figure 15. Measured reactive power at point of common coupling (PCC): (**a**) normal; and (**b**) proposed.

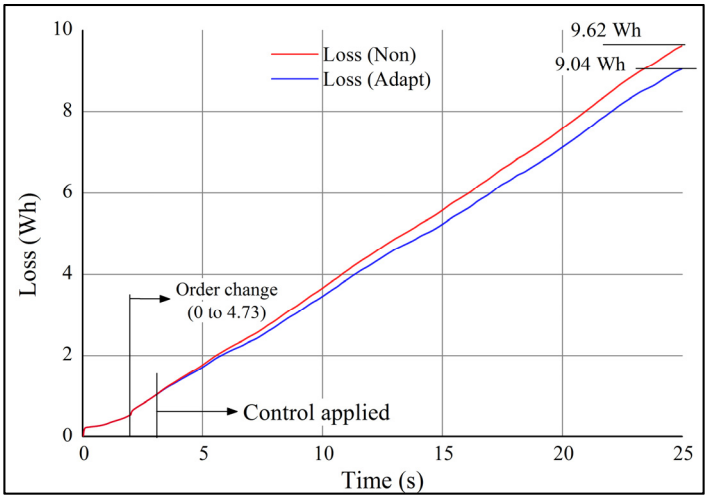

Figure 16. Power loss comparison between both controls.

Table 4. Reference signal for case studies.

Case	Average power loss	Energy loss (25 s)	Absorbed *Q* at PCC
Non-adapted	1.411 kW	9.62 Wh	4.73 MVar
Adapted	1.316 kW	9.04 Wh	4.73 MVar
Improvement	6.7%	6.02%	-

5. Conclusions

This paper suggests a new power control algorithm for the HGS to achieve an optimization process for the inner system's power flow. Through case studies, it is verified that the proposed algorithm contributes to the system efficiency while satisfying the reactive power reliability demands. Owing to the continuous change of active power flow by generation systems, the control scheme changes the reference signal to ensure the current flow balance. The impact of the algorithm would be significant when considering the entire life cycle of the general renewable energy source. As the application of a real time monitoring system, these current flow management methods can generate additional benefits to the operator, and further reactive power reserves can be utilized for the integrated power system.

Acknowledgments

This work was supported by the MOF grant (Development of the design technologies for a 10 MW class wave and offshore wind hybrid power generation system and establishment of the sea test infra-structure) and by Human Resources Development of KETEP grant (No. 20134030200340) funded by the Korea government Ministry of Knowledge Economy.

Conflicts of Interest

The authors declare no conflict of interest.

References

1. Morales, A.; Robe, X.; Sala, M.; Prats, P.; Aguerri, C.; Torres, E. Advanced grid requirements for the integration of wind farms into the Spanish transmission system. *IET Renew. Power Gener.* **2008**, *2*, 47–57.
2. Muyeen, S.M.; Takahashi, R.; Murata, T.; Tamura, J. A Variable speed wind turbine control strategy to meet wind farm grid code requirements. *IEEE Trans. Power Syst.* **2010**, *25*, 331–340.
3. Yun-Hyuk, C.; Sang-Gyun, K.; Byongjun, L. Coordinated Voltage-Reactive Power Control Schemes Based on PMU Measurement at Automated Substations. *J. Electr. Eng. Technol.* **2015**, *10*, 1400–1407.
4. Hartmann, B.; Dan, A. Cooperation of a grid-connected wind farm and an energy storage unit—Demonstration of a simulation tool. *IEEE Trans. Sustain. Energy* **2012**, *3*, 49–56.
5. Dicorato, M.; Forte, G.; Trovato, M. Voltage compensation for wind integration in power systems. In Proceedings of the 2012 3rd IEEE International Symposium on Power Electronics for Distributed Generation Systems (PEDG), Aalborg, Danmark, 25–28 June 2012; pp. 464–469.
6. Seungmin, J.; Hyun-Wook, K.; Gilsoo, J. Adaptive power control method considering reactive power reserve for wave-offshore hybrid power generator system. *Energy Procedia* **2014**, *61*, 1703–1706.
7. Pérez-Collazo, C.; Greaves, D.; Iglesias, G. A review of combined wave and offshore wind energy. *Renew. Sustain. Energy Rev.* **2015**, *42*, 141–153.
8. Majumder, R. Aspect of voltage stability and reactive power support in active distribution. *Gener. Transm. Distrib. IET* **2014**, *8*, 442–450.
9. Zhao, C.; Guo, C. Complete-independent control strategy of active and reactive power for VSC based HVDC system. In Proceedings of the IEEE Power & Energy Society General Meeting, Calgary, AB, Canada, 26–30 July 2009; pp. 1–6.
10. Senturk, O.S.; Helle, L.; Rodriguez, P.; Teodorescu, R. Power capability investigation based on electrothermal models of press-pack IGBT three-level NPC and ANPC VSCs for multimegawatt wind turbines. *IEEE Trans. Power Electron.* **2012**, *27*, 3195–3206.
11. Tian, J.; Su, C.; Soltani, M.; Chen, Z. Active power dispatch method for a wind farm central controller considering wake effect. In Proceedings of the IEEE Conference on Industrial Electronics Society, Dallas, TX, USA, 29 October–1 November 2014; pp. 5450–5456.
12. Rosyadi, M.; Muyeen, S.M.; Takahashi, R.; Tamura, J. Voltage stability control of wind farm using PMSG based variable speed wind turbine. In Proceedings of the 2012 International Conference on Electrical Machines (ICEM), Marseille, France, 2–5 September 2012; pp. 2192–2197.
13. Beerens, J. Offshore hybrid wind-wave energy converter system. Master's Thesis, Delft University of Technology, Delft, The Netherlands, 26 February 2010.
14. Chunhua, L.; Chau, K.T.; Lee, C.H.; Fei, L. An efficient offshore wind-wave hybrid generation system using direct-drive multitoothed rotating and linear machines. In Proceedings of the 2014 17th International Conference on Electrical Machines and Systems (ICEMS), Hangzhou, Zhejiang, China, 22–25 October 2014; pp. 273–279.
15. Rekola, J.; Tuusa, H. Comparison of line and load converter topologies in a bipolar LVDC distribution. In Proceedings of the 2011 14th European Conference on Power Electronics and Applications, Birmingham, UK, 30 August–1 September 2011; pp. 1–10.

16. Ullah, N.R.; Bhattacharya, K.; Thiringer, T. Wind farms as reactive power ancillary service providers—Technical and economic issues. *IEEE Trans. Energy Convers.* **2009**, *24*, 661–672.
17. Barthelmie, R.J.; Hansen, K.S.; Pryor, S.C. Meteorological controls on wind turbine wakes. *IEEE Proc.* **2013**, *101*, 1010–1019.
18. Hyeon-Jae, S.; Jang-Young, C.; Yu-Seop, P.; Min-Mo, K.; Seok-Myeong, J.; Hyungsuk, H. Electromagnetic vibration analysis and measurements of double-sided axial-flux permanent magnet generator with slotless stator. *IEEE Trans. Magn.* **2014**, *50*, 1–4.
19. Bunjongjit, K.; Kumsuwan, Y.; Sriuthaisiriwong, Y. An implementation of three-level BTB NPC voltage source converter based-PMSG wind energy conversion system. In Proceedings of the TENCON 2014-2014 IEEE Region 10 Conference, Bangkok, Thailand, 22–25 October 2014; pp. 1–5.